Memory Devices and A/D Interfaces: Design Trade-offs in Mixed-Signal Accelerators for Machine Learning Applications

Original
Memory Devices and A/D Interfaces: Design Trade-offs in Mixed-Signal Accelerators for Machine Learning Applications / Caselli, Michele; Debacker, Peter; Boni, Andrea. - In: IEEE TRANSACTIONS ON CIRCUITS AND SYSTEMS. II, EXPRESS BRIEFS. - ISSN 1549-7747. - 69:7(2022), pp. 3084-3089. [10.1109/TCSII.2022.3174622]

Availability:
This version is available at: 11381/2923529 since: 2022-07-26T13:20:15Z

Publisher:
IEEE

Published
DOI:10.1109/TCSII.2022.3174622

RSSI-Based Indoor Localization and Identification for ZigBee Wireless Sensor Networks in Smart Homes

Valentina Bianchi, Paolo Ciampolini, and Ilaria De Munari

***Abstract*— Location-based services have increased in popularity in recent years and can be fruitfully exploited in the field of smart homes, opening the doors to a wide range of personalized services. In this context, radio technology can be widely employed since, other than connecting devices in the home system, it offers solutions for the user localization issue without the need of any extra device. Techniques based on received signal strength indicator (RSSI) are often used, relying on fingerprinting or proximity algorithms. In this paper, a novel RSSI-based fingerprinting approach for room-level localization is presented: it is a threshold algorithm based on receiver operating characteristic analysis. Moreover, the actual user location is estimated from his/her interaction with the home system devices deployed in the house: if the home environment is inhabited by more than one person, it becomes of utmost importance the identification of who is actually interacting with a given device. A proximity method is exploited for this purpose. Tests have been carried out to characterize the approach, particularly, the effects of RSSI samples, number and position, of the anchor nodes have been analyzed. Finally, some considerations about power consumption of the mobile node have been presented.**

***Index Terms*— Ambient-assisted living (AAL), home automation system, identification, localization, received signal strength indicator (RSSI), smart homes, wearable device, wireless sensors network, ZigBee.**

I. INTRODUCTION

SMART homes have been traditionally conceived for automation and convenience; in recent years, home systems have been enhanced with more intelligent features to add benefits in a large number of other fields. Among these, the ambient-assisted living (AAL) context has particular importance [1]. One of the aims of AAL technologies [2], [3] is to create better conditions of life for older adults encouraging independence and self-confidence. Research interests focus on monitoring the environment and registering the user's actions to detect dangerous situations for the occupants or more generally to infer patterns and make predictions. The system can perform some actions automatically, freeing the users from manual control, and at the same time, it can implement behavioral analysis (BA) to detect anomalies in the habits requiring particular attention, improving the users' sense of safety [4]. These services can be enhanced by the information about the user location. As an example, for security and safety purposes, it is of crucial importance to detect whether the person is near a hazardous area (e.g., leaving the apartment, being alone in the bathroom, and so on) or in the case of a dangerous event such as a fall, knowing in which area it happened [5]. In this context, a coarse estimation of the user position (e.g., room level) is often sufficient; moreover, it is worth considering that an accurate localization can be automatically carried out by detecting the interaction of the user with the devices that are part of the automation system and are deployed in the house, having a known and fixed position. In this regard, especially for BA purposes, in an environment populated by more than one end user, some strategies must be implemented to identify the actual user who interacted with a given sensor. In this sense, we can refer to the user identification as an indirect localization method.

The services described earlier are location-based services (LBSs): according to their definition [6], they are "services that use the location of the target for adding value to the service," e.g., "automatically activating the service when a target enters or leaves a predefined location."

The LBSs have increased in popularity over recent years and more consumer goods such as mobile phones and wearable devices include a feature for locating the user [7], [8]. Outdoor, satellite navigation systems (e.g., GPS [9], Galileo [10], GLONASS [11], and BeiDou [12]) can provide a high-accurate positioning, but satellite signals are not available indoor resulting in a very poor location. Therefore, some other systems must be investigated to provide user location inside a building. Currently, the commonly adopted indoor localization techniques include Wi-Fi [13]–[15], Bluetooth [16], ZigBee [17]–[19], ultrawideband [20]–[22], radio-frequency identification (RFID) devices [23], and visual sensors [24]. The latter two technologies are often adopted also for user identification [25], but vision involves well-known robustness and scalability challenges while RFID devices suffer from limitations in the reading range, thus relying on user awareness and cooperation. In addition, dedicated hardware is needed for both visual sensors and RFID management, which results in higher implementation costs. This makes these techniques not fully suitable for general applications, and solutions based on more diffused technologies are to be preferred [26].

Manuscript received February 5, 2018; revised May 24, 2018; accepted June 14, 2018. This work was supported by the European Union's AAL Programme through the HELICOPTER Project under Grant AAL-2012-5-150 and the ENSAFE Project under Grant AAL-2014-1-112. The Associate Editor coordinating the review process was Dr. Serge Demidenko. *(Corresponding author: Valentina Bianchi.)*

The authors are with the Department of Engineering and Architecture, University of Parma, 43124 Parma, Italy (e-mail: valentina.bianchi@unipr.it; paolo.ciampolini@unipr.it; ilaria.demunari@unipr.it).

Color versions of one or more of the figures in this paper are available online at http://ieeexplore.ieee.org.

Digital Object Identifier 10.1109/TIM.2018.2851675

In this paper, we describe a ZigBee-based solution for both coarse/room-level localization and user identification. The advantage of the ZigBee solution is that no other hardware or specific configuration is needed with respect to that already deployed for the other features of the home automation system.

We propose a novel algorithm, fusing fingerprinting and proximity techniques: performance of this solution will be discussed and related to practical implementation on real environments.

This paper is organized as follows. In Section II, the state of the art in the field of indoor localization is presented, and the proposed method is introduced. In Section III, the hardware devices used to test the proposed method are described. In Section IV, the proposed method is further detailed, and the system performance is evaluated. In Section V, the conclusions are drawn.

II. Related Works

Indoor localization techniques often use fingerprinting (scene analysis) or proximity algorithms [27], [28]. Fingerprinting algorithms [29], [30] consist of two phases: in the first one (training phase), some features (fingerprints) of the environment are collected, and in a second phase (run phase), they are matched with the online measurements to extrapolate the mobile object position. The most basic proximity algorithms rely on detecting human physical contact [27]. Other examples of proximity algorithms are usually used for room-level localization and rely on a set of antenna having a known position (the so-called anchor nodes). When a mobile target is in the range of one antenna, it is considered to be in the same area, while when more than one antenna is involved, the one receiving the highest signal level is selected [28].

The ZigBee solutions are often based on received signal strength indicator (RSSI) approaches [31]–[35]: an RSSI can be obtained for each ZigBee message and can be correlated with the distance between the two transceivers involved in the communication. The distance $d_{i,j}$ between a given transceiver couple (i, j) can be related to an RSSI by the simple relationship [36]

$$\mathrm{RSSI}_{i,j} = -m\log\left(d_{i,j}\right) + C \tag{1}$$

where m is a constant involving signal propagation features, related to the actual signal path and C is a fixed constant.

RSSI can be used as a metric in both fingerprinting and proximity algorithms. The latter are usually simpler to implement, but in a real environment, due to scattering phenomena into the propagation signal path [37], it is not straightforward that the difference between two RSSIs from two devices in different locations is easily predictable, so a fingerprinting is often actually necessary.

In this paper, we propose a localization algorithm exploiting both fingerprinting and proximity techniques. A coarse, room level, user localization is carried out using a threshold-based fingerprinting matching algorithm exploiting a novel receiver operating characteristic (ROC) analysis method. ROC curves are usually used to evaluate the classification system performance. In this paper, we use them not only to evaluate the system performance in response to some parameters change (i.e., anchor nodes position or the number of RSSI measurements) but also, as a method, used in the training phase, to compute a threshold (peculiar to each environment) exploited into the online phase to discriminate in which room the user is. Moreover, precise user's position can be assessed considering his/her interaction with a given sensor, deployed into the home environment. In this case, considering that more than one user can actually live in the home, an identification feature is needed: to identify the user, we exploit an RSSI proximity-based algorithm.

In [38]–[43], similar experiments are reported, exploiting fingerprinting techniques with different metrics. In [38], a room-level RSSI-based approach has been presented and an accuracy of 93% is achieved. No details on the number of RSSI samples and mobile node power consumption are reported. In [39], a room-level threshold-based algorithm is presented. The thresholds are computed taking into account the size of the rooms and some RSSI measurements. No details on the number of RSSI measures used to calibrate the propagation model in the training phase are given. They obtain an averaged accuracy of 90.1% and 94.4% into a home and office environment, respectively. They use 10 RSSI measurements: no analysis is carried out on the influence of the number of RSSI measures on the accuracy obtained or the power consumption of the mobile node. In [40], an algorithm based on the heuristic passing through a boundary point between two rooms (e.g., an entrance door) is reported. Although a good accuracy of 97.1% is achieved, a standard method to reproduce the training set in other environments is not discussed: 200 RSSI measures for each room plus 100 measures for each doorway have been collected, but an analysis of the influence of these numbers on the gained accuracy and some details about the positions in which measurements are collected is not presented. Moreover, the number of RSSI samples needed in the training phase is quite high: this increases the installation burden, limiting the general adoption of the system. In [41] and [42], occupancy detection approaches, exploiting i-Beacon technology, have been proposed. Data are elaborated through support vector machine classification models. Corna *et al.* [41] achieve an accuracy of 94%; Barsocchi *et al.* [42] exploit a multipower approach: the RSSI values have been collected considering three different time windows (1, 2.5, and 5 s) and accuracies of 92.5%, 96.4%, and 98.1% have been, respectively, obtained. In [43], an occupancy detection strategy, exploiting a completely different technology, has been proposed. The authors analyzed data from some environmental sensors (light, temperature, humidity, and CO_2): the best result, 98% of accuracy, has been reached elaborating data from the light sensor, applying a classification and regression trees model. The time response of this system is, however, quite high, since data have been acquired and averaged over a window of one minute. Candanedo and Feldheim [43] suggest that this good result could be related to "higher sensor's accuracies, resolution, and/or sensor location"; however, a study on the sensor position is not reported. Moreover, since the aim in [43] is to implement smart energy management strategies, the identification of the user is not of particular interest, and therefore, the approach described does not implement this feature. However, if the aim of the system is to monitor the users' behavior, the identity of the person inside the room is significant, especially when more people are living in the same home.

Comparing to these works, we demonstrate that it is possible to obtain, with the proposed ROC-based method and with only one anchor node per room, an accuracy equal to 98%, over a time window of 1 s, without exploiting specific sensors, but only the nodes of the system infrastructure and a personal wearable sensor. Exploiting the interaction with some sensors deployed in the house at a fixed location for behavioral monitoring purposes, the exact position of the user can be also inferred. Moreover, in this paper, we analyze the effect on the algorithm performance of multiple RSSI samples, anchor node position and number, aiming at providing some indications to a practical deployment of such a system in a real home environment, minimizing the number of RSSI measures needed during the training phase and then the installation burden and costs. Finally, some considerations about the increase in power consumption due to the localization and identification features in the mobile node are reported.

To collect the RSSI measures and test the proposed solution a ZigBee home automation system named Computer-Aided, Rule-based system for Domestic Environment Assistance (CARDEA) [44], developed at the University of Parma, has been exploited. The hardware devices designed for the system and used in this paper are described in Section III.

III. Hardware Devices

CARDEA system merges environmental sensor functions and wearable sensor for personal monitoring in the same framework.

Environmental sensors provide data related to the user's interaction with the home environment. Examples of these sensors are room presence sensors, bed or chair occupancy sensors, fridge and cupboard sensors (to monitor feeding habits), toilet sensors, and power meters (to monitor appliances usage; e.g., TV set). Wearable devices provide information about individual physical activity, also enabling fall detection and emergency button services.

All devices are based on the ZigBee/IEEE 802.15.4 protocol because of its low cost and low power consumption. CARDEA system takes advantage of the ZigBee PRO version, in particular for the stochastic addressing and the "many to one source routing" features [45].

Hence, devices for creation and management of a standard ZigBee network (i.e., network coordinator and routers) are also present. In the localization method proposed in this paper, standard routers act as beacons in the room-level localization feature, while the environmental sensors are exploited during the identification phase, in the proximity technique.

To keep the implementation costs limited, three printed circuit board (PCB) modules [46] have been designed, to be configured and assembled in different ways, to implement a complete devices family, both wearables and environmental, as well as networking gear (the network coordinator and router nodes).

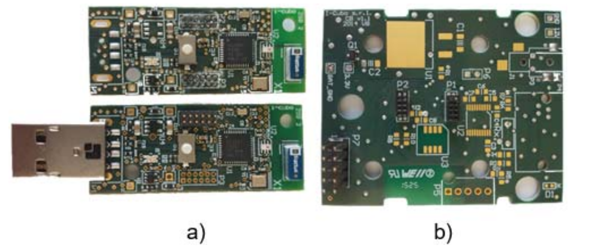

Fig. 1. PCBs. (a) Environmental sensors radio module (top) and coordinator/routers (bottom). (b) Environmental sensors carrier board.

The three basic modules (Fig. 1) are described in the following.

A. Radio Module

A common board has been designed to equip both the networking elements and the environmental sensors. The coordinator, that acts also as the bridge between the ZigBee network and the home gateway, and the routers were conceived as universal serial bus (USB) sticks, thus resulting in the 19 mm $\times$ 45 mm configurable board shown in Fig. 1(a). It is a four-layer board, featuring four functional sections: the core, the antenna, the power, and the I/O section.

1) Core Section: It is based on the CC2531 SoC by Texas Instruments, which embeds an 8051 8-bit microcontroller unit. It deals with both the Zigbee stack management and onboard data processing. It integrates a USB port and three general-purpose I/O ports, which can be exploited for physical sensor interfacing.

2) Antenna Section: As already explained, signal propagation properties are exploited to estimate distance among interacting nodes, in order to implement the identification and localization features. Therefore, an antenna radiation diagram as omnidirectional as possible is required, not to introduce artifacts in such a process. This, together with miniaturization constraints, led us to avoid printed antennas and to select a chip antenna: Fractus Reach Xtend [47] chip has been selected. The antenna circuit is matched against the core circuit by using an integrated Balun by Johanson Technology [48]. Care was taken in the PCB design to keep the area around the antenna free from ground planes and other interfering objects, and to keep connecting paths as short as possible.

3) Power Section: The core section requires a supply voltage in the 3–5-V range. Depending on the actual configuration, different power sources have been employed, when used as router or coordinator, the board is powered (5 V) via the USB port, whereas environmental sensors are typically battery powered (3 V). Therefore, an optional dc–dc converter is mounted on the board in the former case, whereas batteries can be straightforwardly connected to through-hole pads.

4) I/O Section: Available pins are exploited according to the actual needs, depending on the board destination. A couple of LEDs and a reset button are present anyway. Then, coordinator and router implementations require mounting the USB connector. If the board fits environmental sensors instead, two connectors are mounted for coupling to the sensor "carrier" board [Fig. 1(b)], the physical interface between different sensors and the common radio and processing module.

This article has been accepted for inclusion in a future issue of this journal. Content is final as presented, with the exception of pagination.

Fig. 2. MuSA wearable sensor.

Also, an operational-amplifier buffer is mounted, to allow for interfacing analog sensors through the CC2531 internal Analog-to-Digital Converter. Different types of sensors have been implemented, interfacing the appropriate sensitive element:

1) chair/bed sensor (pressure pad as a sensitive element);
2) presence sensor (passive infrared);
3) fridge/cupboard sensor (photoresistance and temperature and humidity sensor);
4) toilet sensor (distance sensor);
5) door/window opening (magnetic contact).

B. Wearable Device Board

It exploits the same architectures introduced earlier for the radio and processing module, but it has been redesigned considering ergonomic constraints: size and weight have to be minimized, to reduce the user's burden. In Fig. 2, a view of the MUltiSensor Assistant (MuSA) device [49], [50] is shown.

The device is aimed at monitoring user's motion, detecting falls and evaluating energy expenditure. It also features an "emergency call" button. Depending on the actual purpose, it can be worn on the user's belt, in the pocket, at the wrist, or as a necklace pendant.

The PCB is a four-layer board and can be divided into five sections:

1) Core Section: Similarly, to the home sensors introduced before, the board exploits the TI-CC2531 SoC to manage radio communication and onboard data processing.

2) Antenna Section: The same chip antenna is exploited, and similar design consideration applies.

3) Power Section: A tiny, rechargeable Li-ion battery is exploited. It supplies a nominal voltage of 4.2 V, so that a dc–dc converter is needed to power the CC2531-based core module. A battery charger circuit, based on the BQ24400 chip by Texas Instruments, is implemented as well, complemented by a TPS63031 buck–boost converter, which allows exploiting at best the full battery charge.

4) Sensors Section: The board is conceived as a multisensor platform and can be configured on purpose at assembly time. It mounts an ST-LSM9DS0 inertial measurement unit (IMU), which features a 3-D accelerometer, gyroscope, and magnetometer, integrated into a single chip. The IMU provides information about user motion, depending on the firmware algorithm.

5) I/O Section: A couple of LEDs are used for communicating the device status. The USB port (through a standard micro-USB connector) is exploited to power the device, recharge the battery, and communicate "off-line" data. A membrane keyboard has been designed, which integrates two buttons. One is used for control purposes (turning the device ON and OFF, or configuration tasks) and the other allows for the emergency call function.

All of these PCBs have been successfully tested for electromagnetic compatibility issues, qualifying for Conformité Européenne certification.

IV. Proposed Localization Method

The ZigBee system has been exploited to test and characterize the proposed localization techniques. Considering that each user wears a MuSA device, that in turn inherently brings information about his/her identity, and that the ZigBee routers can be used also as a radio beacon, the user position can be assessed through the RSSIs collected from the messages exchanged between the devices. A coarse localization technique based on a fingerprinting solution is used to assess in which room the user is, while the actual user's position can be inferred from his/her interaction with the system devices deployed in the house. For this purpose, it is possible to assume that the user actually interacting with a given sensor is (among possible many present in the same room) the one who is closest to the sensor itself. Based on this, in environments populated by more than one end user, the identification mechanism can also be devised: every time an environmental sensor is activated, it polls all wearable devices within the home, and compares the RSSIs from different users. The user wearing the device that features the highest RSSI is identified as the one actually interacting.

The environmental sensors equipped with the identification feature are conceived for an individual user (i.e., toilet sensor, chair sensor, door sensor, and fridge/cupboard sensor), so the possibility of more than one user interacting with the same device was not taken into account. The system has been tested considering a minimum distance of one meter from a user to another.

Since both localization and identification features do not involve additional hardware components, we, therefore, implemented such features into the firmware of all sensors in the network: details about testing and performance of the proposed solution are given in Sections IV-A–IV-D.

A. Setup of the Test Environment

The system performance was evaluated through some laboratory tests simulating a real environment (Fig. 3).

In rooms A and C (both about 40 m^2), a matrix of 25 measurement points was considered, while in room B only five positions have been taken into account, due to the smaller dimension of the corridor. An identification number indicates each measurement point. The wearable sensors generate signals that are received by beacons (i.e., routers described in Section III) or by environmental sensors (depending on the feature that is under test) and from which an RSSI measure can be extracted.

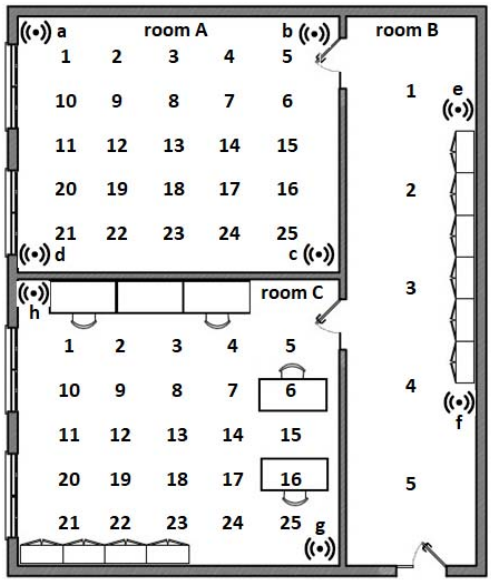

Fig. 3. Test environment.

In the following paragraphs, details are given about the characterization and the performance of the localization and identification techniques.

B. Localization Feature

The localization algorithm relies on an RSSI-based fingerprinting technique. In the training phase, repeated measures of the received power are necessary to build a map of the specific environment peculiarities that induce scattering phenomena and modify RSSIs along a given trajectory. Then, in the run phase, the collected values during normal daily living activities are compared to the off-line measures to estimate the user location. The training phase may obviously complicate the installation of the system. Therefore, it is necessary to provide a method that limits both the number of measurement points and the number of measures in each point and provides an indication on the beacons optimal position (i.e., the position that guarantees the best accuracy for the localization feature). In some situations, a large number of beacons can provide greater accuracy; however, it affects the cost of the entire system and its deployment. For this reason, considering that the target is to localize the user in an area (i.e., a room), a beacon per room has been considered.

Intuitively, a good positioning criterion might be used to place the beacons far from adjacent rooms. To verify this, a total of eight beacons (indicated with a, b, c, d, e, f, g, and h) were deployed in the laboratory environment as depicted in Fig. 3.

To measure how the beacon location impacts on the system performance in terms of sensitivity and specificity Fawcett's ROC theory has been exploited [51]. Considering a beacon, the user positions inside the room in which the beacon is being evaluated as positive instances, while those external are negative ones.

From the ROC curves, it is possible to analyze the sensitivity and the specificity of the system defined as

$$\text{sensitivity} = \frac{\text{TP}}{\text{TP} + \text{FN}} \tag{2}$$

TABLE I

DEFINITION OF TP, TN, FP, AND FN

Symbol		room in which the user is	room in which the user is identified
TP	(True Positive)	A	A
TN	(True Negative)	B or C	not in A
FP	(False Positive)	B or C	A
FN	(False Negative)	A	not in A

TP, TN, FP and FN are here defined with reference to beacon "a" in the room "A". Equivalent definitions can be reported with respect to the other beacons

$$\text{specificity} = \frac{\text{TN}}{\text{FP} + \text{TN}} \tag{3}$$

where TP, FN, TN, and FP are defined in Table I.

The sensitivity represents the rate of true positives; it, therefore, describes the system capability to correctly identify a positive value. On the contrary, specificity is related to the rate of true negatives.

The mean over 300 RSSIs for each of the 55 positions indicated in Fig. 3 was carried out and sorted in a decreasing order. The ROC curves for the eight beacons have been calculated and they are shown in Fig. 4.

These plots have been obtained following the method described in [51]: the samples are placed into the ROC graph according to their class belonging (positive/negative instances). Since the x-axis of the ROC curve represents "1-specificity" and the y-axis represents the sensitivity, the bigger the area under the curve the better the performance of the system.

From Fig. 4, it is confirmed that the beacons far from the boundaries with other rooms are the best candidate for an accurate user localization; we, therefore, selected beacon a, e, and g for the subsequent tests.

Then, the minimum number of measurements in the training phase has to be evaluated.

In order to keep the number of training position low (and thus to limit the installation burden), in each room, a subset of positions has been selected. To make these positions representative of the whole room, the positions in the corners (or at the ends in the case of room B) and in the middle of the rooms has been chosen. In Table II, the selected positions (according to those defined in Fig. 3) for each room have been reported.

For each position, k RSSIs (with k equal to 1, 10, 20, 30, 40, and 50) have been sampled from the set of 300 measurements carried out to characterize beacon position. The mean of the RSSIs gathered has been computed and an ROC curve is carried out for each k. This experiment has been repeated 1000 times to acquire statistical significance.

The frequency of the k trials with a given sensitivity for a specificity of 100% is shown in Fig. 5. On the x-axis, the sensitivity (in percentage) is reported. The optimal ROC curve is obtained with a sensitivity equal to 100%.

Averaging over 50 RSSI samples guarantees a good accuracy of the approach. Considering that the time interval between two RSSI measurements has been estimated in 100 ms, the duration of the training phase in our example with 13 positions is about 10 min (considering also the time for the user to move from a position to another one) and it is

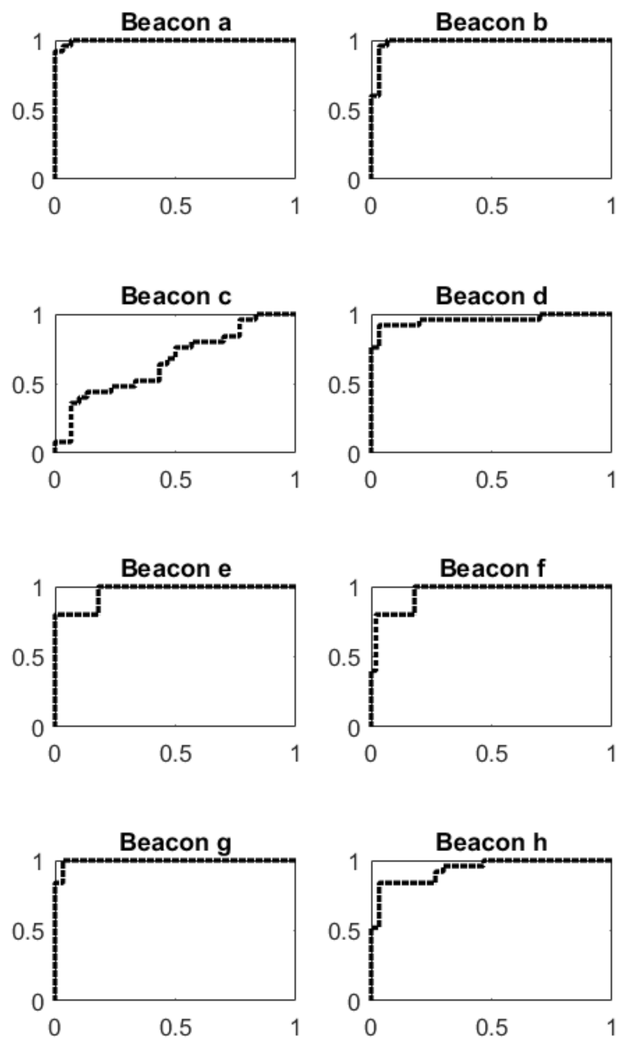

Fig. 4. ROC curves for the eigth beacons. For each plot, the x-axis represents "1—specificity," while the y-axis represents the sensitivity.

TABLE II

POSITIONS SELECTED FOR THE TRAINING PHASE

Room	Position number
A	1,5,13,21,25
B	26,28,30
C	31,35,43,51,55

definitely acceptable. Obviously, the actual assessment of the user position during daily living activities cannot rely on a such number of measurements: to obtain a much faster localization, the number of samples during the live phase is reduced to 10: this ensure that the time spent to locate the user is only 1 s.

Exploiting ROC curve during the training phase has another important advantage: it allows to intrinsically carry out a threshold value that is appropriate to discriminate in which room the user is. Once the RSSIs are sorted to compute the RSSI curve, the selected threshold will be the RSSI value that best manages to properly separate the positive instances from the negative ones. This threshold somehow describes the peculiarities of signal propagation in a specific environment,

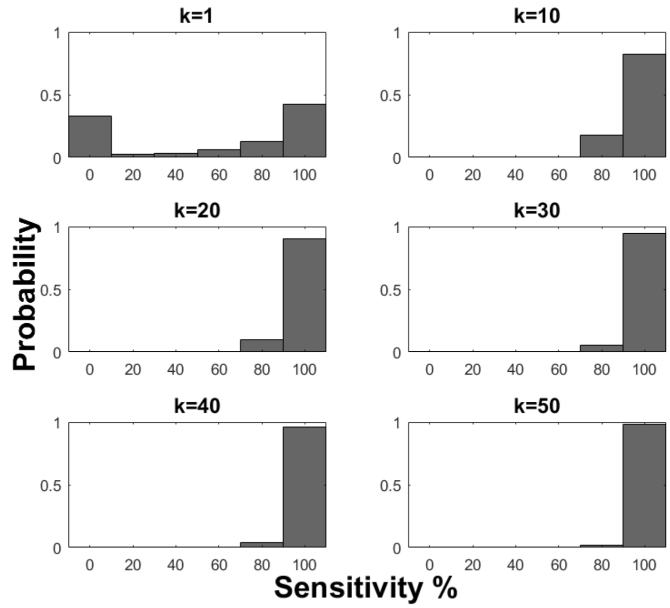

Fig. 5. Probability of obtaining a given sensitivity for a specificity of 100%.

and it is related to the room in which it is computed. In order to determine the position of the user in the environment, the parameter D_x has been considered

$$D_x = \mathrm{RSSI}_m - \mathrm{th}_x \tag{4}$$

where th_x is the threshold carried out in the training phase for the beacon x, the RSSI_m is the mean of the RSSI computed in the run phase, and D_x the difference between RSSI_m and the threshold related to the beacon x. In the run phase, the user will be assigned to the room with the beacon that shows the greater D_x value.

Some tests have been set up to evaluate the whole procedure. A training phase has been performed considering 50 RSSI measurements in the 13 sample points defined earlier, five in rooms A and C and three in room B. An ROC curve and a threshold have been carried out for the three selected beacons (and then for the three rooms), and they are reported in Fig. 6.

In the run phase, 10 measurements are sampled for each of the 55 positions and then averaged. According to (4), D_x is carried out for each beacon and it is evaluated to assign the user to a room. This is repeated for 1000 times in order to assess the performance of the method, in terms of sensitivity, specificity, and accuracy. The latter is defined as

$$\text{accuracy} = \frac{\mathrm{TP} + \mathrm{TN}}{\mathrm{TP} + \mathrm{TN} + \mathrm{FP} + \mathrm{FN}}. \tag{5}$$

To consider only fair statistics (i.e., cases with positive instance number quite similar to the negatives one), we analyze the case of room A occupancy and room C occupancy. The related system performance is reported in Table III.

These statistics result in an overall accuracy of 98.2%.

In order to better evaluate the performance of the proposed method, another metric has been evaluated using the maximum RSSI: in this case, the user is assigned to the room in which the beacon receiving the maximum RSSI is located. With this algorithm, an accuracy of 85% in the case of

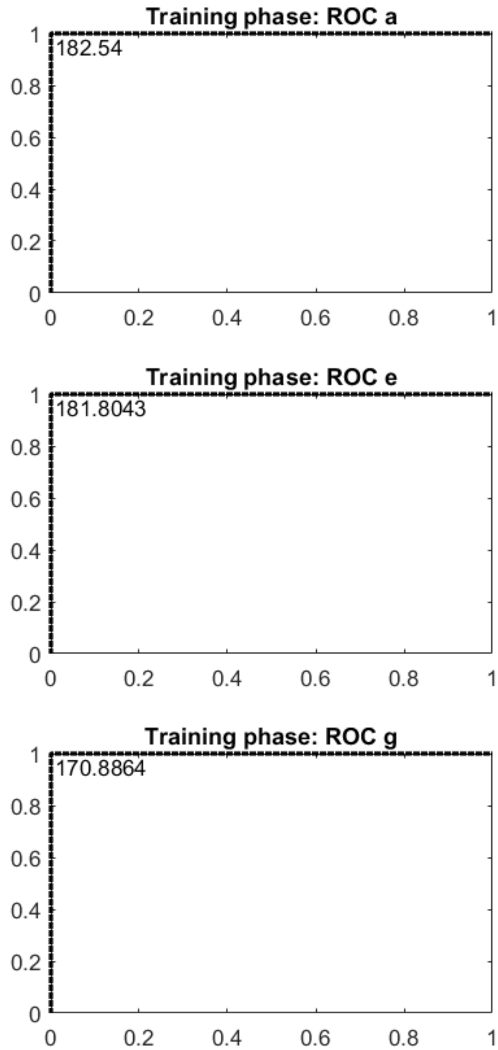

Fig. 6. ROC curve computed in training phase for selected beacons, with associated threshold.

TABLE III
PERFORMANCE OF LOCALIZATION FEATURE

Room Occupancy	Accuracy	Sensitivity	Specificity
Room A	98.2%	96%	100%
Room C	98.2%	100%	96.7%

room A occupancy and 87% for room C, has been obtained. This can be explained considering the differences between the environments that affect the signal propagation. If, for example, for a particular beacon, the RSSI values are generally lower, a threshold approach can consider it, resulting in a better performance.

C. Tests and Characterization: Identification

The same environment has been exploited also to assess the performance of the action tagging strategy.

The test procedure is the following: we replaced the beacon *c* with a ZigBee environmental device, according to Fig. 3, and then two people wearing their own MuSA wearable device have been considered. The first one (U_1) stands close to the sensor (position 25), while the second one (U_2) moves at the other locations into the environment. Different positions for the sensor and user U_1 were tested; here, we refer to the "worst case" test, in which the sensor node is in a position that maximizes the chances of misinterpretation (considering adjacent rooms).

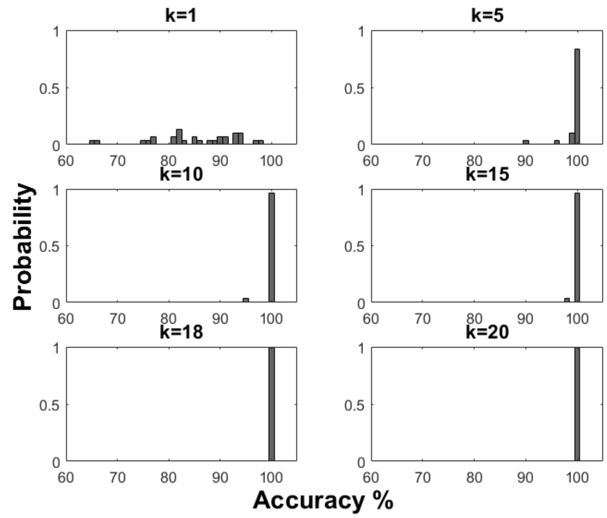

Fig. 7. Probability of obtaining given accuracy during identification task.

Other sensor positions tested, although yielded better results than those illustrated in the following.

The test aims at evaluating the identification accuracy, i.e., checking how reliably the procedure correctly identifies the closest user (U_1). As in the case of localization, the use of a "single-shot" RSSI measurement, it is not reliable: a good accuracy in identifying the user can be obtained only averaging k samples and using the mean in the comparison. This concept is illustrated in Fig 7: the probability of obtaining a given degree of accuracy (i.e., the number of tests in which the user U_1 is correctly identified versus the total number of tests, over all 55 positions) varying the number of samples, is reported.

As shown earlier, the tests with $k = 1$ are far from being satisfactory, as expected, due to the nonidealities in the room, with several trials reporting accuracy well below 80%. This can be better appreciated by looking at the box diagrams of the distributions of the two set of measurements: in Fig. 8, it is shown that U_1 and U_2 RSSI distributions may actually overlap, and it is possible that a measure of set U_2 results greater than corresponding one in set U_1, thus causing a false attribution.

Selecting k value larger than 15 guarantees good results and it is fully compatible with practical implementation. We need to keep the procedure short enough with respect to the action to be tagged (not to miss shortest events). This results in an upper limitation of k value: assuming a maximum procedure duration of 2 s (which is suitable for the application at hand) and considering a 100-ms time interval between subsequent RSSI samplings, we may account for k up to 20, which yields excellent accuracy already.

However, a larger number of exchanged messages also entail an increased energy consumption. As wearable devices

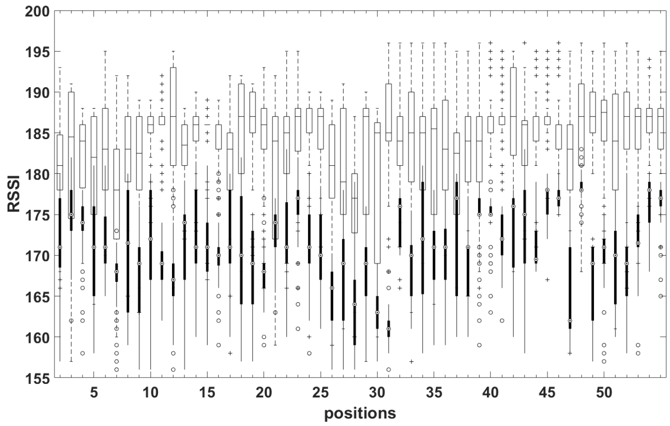

Fig. 8. Box plot of RSSI measurements for user A (unfilled boxes) and user B (filled boxes). Cross markers represent outliers.

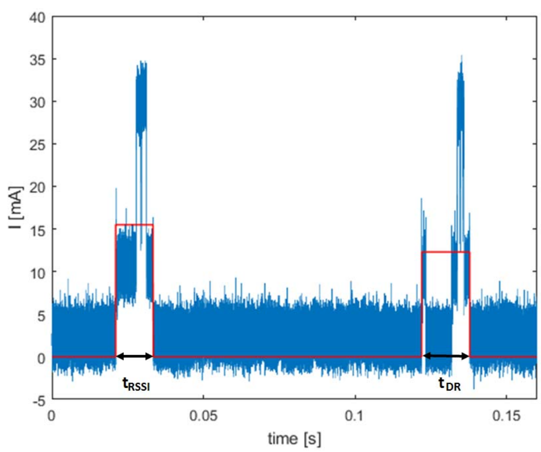

Fig. 9. Measurement of MuSA sensor current.

are battery powered this could lead to a shortening of the device lifetime. In Section IV-D, some considerations about this matter are reported.

D. Energy Considerations

According to the ZigBee protocol specifications, each message sent from an end device (such as the MuSA platform) need to be followed by a "data request" (DR) message, to check for pending messages. If messages are closely packed into a 100-ms interval stream, the stack just waits for the end of the stream to issue a new DR. Hence, for a given k, the energy E_{tag} required by the whole procedure can be estimated as follows:

$$E_{\text{tag}} = k \times E_{\text{RSSI}} + E_{\text{DR}} \tag{6}$$

where E_{RSSI} and E_{DR} are the energy required by a single RSSI evaluation and by the DR message, respectively. Such energies can be estimated by measuring the absorbed current by the sensor during corresponding phases. Fig. 9 shows the actual measured current, highlighting RSSI, and DR messages.

From such current, E_{RSSI} and E_{DR} can be evaluated:

$$E_{\text{RSSI}} = \int_{t_{\text{RSSI}}} V_{\text{dd}}\ I dt = 635\ \mu\text{J} \tag{7}$$

$$E_{\text{DR}} = \int_{t_{\text{DR}}} V_{\text{dd}}\ I dt = 642\ \mu\text{J} \tag{8}$$

where V_{dd} is the supply voltage, I is the measured current, t_{RSSI} is the time for sending an RSSI message, and t_{DR} is the time for a DR message.

We can thus correlate the number of sample directly to the energy expense. Assuming, for instance, $k = 10$, as in the case of localization feature, (6) yields

$$E_{\text{tag}_{k10}} = 6.99\ \text{mJ}. \tag{9}$$

We can double this value for the identification feature.

Correlating such figure to the battery lifetime is not straightforward since it mostly depends on the sensors primary tasks and on the frequency of activation of identification/localization procedures. As a rough estimate, if we assume a 500-mAh battery capacity and consider (largely overestimated) one identification and one localization procedure every minute (during daily hours, with events occurring during the sleeping time), we end up with a daily consumption which is in the order of 0.3% of the battery capacity. However, introducing the identification feature may involve a further, indirect increase in energy demand: in fact, in its typical use, the information flow related to the wearable device is mostly unidirectional, with sensor uploading data to the home gateway. When no data are to be received by the sensor, DR messages have basically a keepalive function and their frequency can be rather low. By introducing the action tagging feature, information flow becomes actually bidirectional, with wearable devices receiving polling messages issued by the environmental sensor. In order to ensure suitable responsiveness, DR messages need thus to be issued at a higher frequency than that needed for mere keepalive purpose. If we raise the DR rate at 1 Hz, the cumulative daily overhead introduced by the tagging procedure rises to 0.9% of the battery capacity.

Since, due to other tasks, the MuSA battery lifetime (without the localization/identification feature) is in the order of a few days, it appears that such overhead introduced is actually negligible.

V. Conclusion

In this paper, a novel RSSI-based algorithm for user localization in an environment controlled by a ZigBee home automation system is presented. The user position estimation has been carried out without adding dedicated hardware, lowering the impact on the deployment costs. For the user room-level localization, a fingerprinting method is exploited and a threshold-based algorithm is applied. Due to scattering phenomena on the radio-frequency signal, the threshold values depend on the environmental characteristics. To overcome this problem, a novel method, based on the ROC analysis, has been adopted to compute the thresholds. To calculate the actual user position, instead, the interaction of the user with a given sensor already deployed in the house for BA purposes has been considered. In this case, in environments populated by more than one user, the identification of the person who interacted with the device is of utmost importance. In this regard, an RSSI-based proximity algorithm has been used.

For both localization and identification procedures, it is shown that a straightforward, "one shot," implementation does not provide a suitable accuracy. Averaging techniques are thus implemented, allowing to increase accuracy to the desired level, without impacting to a significant extent on power consumption and battery lifetime. Some considerations about the position of the anchor nodes are also presented. Tests have been carried out and an accuracy of 98% with a sensitivity and specificity higher than 96% has been reached.

REFERENCES

[1] M. Bassoli, V. Bianchi, I. De Munari, and P. Ciampolini, "An IoT approach for an AAL Wi-Fi-based monitoring system," *IEEE Trans. Instrum. Meas.*, vol. 66, no. 12, pp. 3200–3209, Dec. 2017.

[2] C. Siegel and T. E. Dorner, "Information technologies for active and assisted living—Influences to the quality of life of an ageing society," *Int. J. Med. Inform.*, vol. 100, pp. 32–45, Apr. 2017.

[3] G. Marques and R. Pitarma, "An indoor monitoring system for ambient assisted living based on Internet of Things architecture," *Int. J. Environ. Res. Public Health*, vol. 13, no. 11, p. 1152, 2016, doi: 10.3390/ijerph13111152.

[4] A. Losardo, V. Bianchi, F. Grossi, G. Matrella, I. de Munari, and P. Ciampolini, *Web-Enabled Home Assistive Tools* (Assistive Technology Research Series), vol. 29. Amsterdam, The Netherlands: IOS Press, 2011, pp. 448–455.

[5] C.-N. Huang and C.-T. Chan, "A ZigBee-based location-aware fall detection system for improving elderly telecare," *Int. J. Environ. Res. Public Health*, vol. 11, no. 4, pp. 4233–4248, 2014.

[6] A. Küpper, *Location-Based Services: Fundamentals and Operation*. Hoboken, NJ, USA: Wiley, Sep. 2005.

[7] A. Colombo, D. Fontanelli, D. Macii, and L. Palopoli, "Flexible indoor localization and tracking based on a wearable platform and sensor data fusion," *IEEE Trans. Instrum. Meas.*, vol. 63, no. 4, pp. 864–876, Apr. 2014.

[8] J.-H. Huh and K. Seo, "An indoor location-based control system using Bluetooth beacons for IoT systems," *Sensors*, vol. 17, no. 12, p. 2917, 2017, doi: 10.3390/s17122917.

[9] T. Logsdon, *The Navstar Global Positioning System*. Cham, Switzerland: Springer, 1992.

[10] H. L. Trautenberg, T. Weber, and C. Schäfer, "GALILEO system overview," *Acta Astronautica*, vol. 55, nos. 3–9, pp. 643–647, 2004.

[11] V. A. Bartenev, V. V. Malyshev, and M. N. Krasilshikov, "Current GLONASS status, upgrades and prospective," *Air Space Eur.*, vol. 1, no. 2, pp. 56–62, 1999.

[12] S. Hongwei, L. Zhigang, and P. Feng, "Development of satellite navigation in China," in *Proc. IEEE Int. Freq. Control Symp. Joint 21st Eur. Freq. Time Forum*, Geneva, Switzerland. May/Jun. 2007, pp. 297–300.

[13] A. Y. Lee *et al.*, "High accuracy indoor localization with low cost based on wireless LAN, mobile sensors and floor layout," in *Proc. IEEE Int. Conf. Consum. Electron.-Asia (ICCE-Asia)*, Seoul, South Korea, Oct. 2016, pp. 1–6.

[14] Z. Chen, H. Zou, H. Jiang, Q. Zhu, Y. C. Soh, and L. Xie, "Fusion of WiFi, smartphone sensors and landmarks using the Kalman filter for indoor localization," *Sensors*, vol. 15, no. 1, pp. 715–732, Jan. 2015, doi: 10.3390/s150100715.

[15] J. Yoo, K. H. Johansson, and H. J. Kim, "Indoor localization without a prior map by trajectory learning from crowdsourced measurements," *IEEE Trans. Instrum. Meas.*, vol. 66, no. 11, pp. 2825–2835, Nov. 2017.

[16] M. Castillo-Cara, J. Lovón-Melgarejo, G. Bravo-Rocca, L. Orozco-Barbosa, and I. García-Varea, "An empirical study of the transmission power setting for Bluetooth-based indoor localization mechanisms," *Sensors*, vol. 17, no. 6, p. 1318, 2017, doi: 10.3390/s17061318.

[17] C.-W. Ou *et al.*, "A ZigBee position technique for indoor localization based on proximity learning," in *Proc. IEEE Int. Conf. Mechatron. Automat. (ICMA)*, Takamatsu, Japan, Aug. 2017, pp. 875–880.

[18] J. Cheon, H. Hwang, D. Kim, and Y. Jung, "IEEE 802.15.4 ZigBee-based time-of-arrival estimation for wireless sensor networks," *Sensors*, vol. 16, no. 2, p. 203, 2016, doi: 10.3390/s16020203.

[19] G. Santinelli, R. Giglietti, and A. Moschitta, "Self-calibrating indoor positioning system based on ZigBee devices," in *Proc. IEEE Instrum. Meas. Technol. Conf.*, May 2009, pp. 1205–1210.

[20] T. Kaiser *et al.*, "Ultra-wideband wireless systems: A broad overview," *URSI Radio Sci. Bull.*, vol. 2007, no. 320, pp. 25–40, Mar. 2007.

[21] A. De Angelis, S. Dwivedi, and P. Händel, "Characterization of a flexible UWB sensor for indoor localization," *IEEE Trans. Instrum. Meas.*, vol. 62, no. 5, pp. 905–913, May 2013.

[22] Y. Zhou, C. Law, Y. Guan, and F. Chin, "Indoor elliptical localization based on asynchronous UWB range measurement," *IEEE Trans. Instrum. Meas.*, vol. 60, no. 1, pp. 248–257, Jan. 2011.

[23] S. S. Saab and Z. S. Nakad, "A standalone RFID indoor positioning system using passive tags," *IEEE Trans. Ind. Electron.*, vol. 58, no. 5, pp. 1961–1970, May 2011.

[24] S. Se, D. Lowe, and J. Little, "Vision-based mobile robot localization and mapping using scale-invariant features," in *Proc. IEEE Int. Conf. Robot. Automat.*, May 2001, pp. 2051–2058.

[25] R. S. Joshua *et al.*, "RFID-based techniques for human-activity detection," *Commun. ACM*, vol. 48, pp. 39–44, Sep. 2005.

[26] J. Xiong, B.-C. Seet, and J. Symonds, "Human activity inference for ubiquitous RFID-based applications," in *Proc. Symp. Workshops Ubiquitous, Autonomic Trusted Comput.*, Jul. 2009, pp. 304–309.

[27] Z. B. Tariq, D. M. Cheema, M. Z. Kamran, and I. H. Naqvi, "Non-GPS positioning systems: A survey," *ACM Comput. Surv.*, vol. 50, no. 4, Nov. 2017, Art. no. 57.

[28] H. Liu, H. Darabi, P. Banerjee, and J. Liu, "Survey of wireless indoor positioning techniques and systems," *IEEE Trans. Syst., Man, Cybern. C, Appl. Rev.*, vol. 37, no. 6, pp. 1067–1080, Nov. 2007.

[29] M. Raspopoulos, "Multidevice map-constrained fingerprint-based indoor positioning using 3-D ray tracing," *IEEE Trans. Instrum. Meas.*, vol. 67, no. 2, pp. 466–476, Feb. 2017.

[30] P. Mirowski, D. Milioris, P. Whiting, and T. K. Ho, "Probabilistic radio-frequency fingerprinting and localization on the run," *Bell Labs Tech. J.*, vol. 18, no. 4, pp. 111–133, 2014.

[31] H. A. Nguyen, H. Guo, and K.-S. Low, "Real-time estimation of sensor node's position using particle swarm optimization with log-barrier constraint," *IEEE Trans. Instrum. Meas.*, vol. 60, no. 11, pp. 3619–3628, Nov. 2011.

[32] S. K. Gharghan, R. Nordin, and M. Ismail, "A wireless sensor network with soft computing localization techniques for track cycling applications," *Sensors*, vol. 16, no. 8, p. 1043, 2016.

[33] Y. Alvarez and F. L. Heras, "ZigBee-based sensor network for indoor location and tracking applications," *IEEE Latin Amer. Trans.*, vol. 14, no. 7, pp. 3208–3214, Jul. 2016.

[34] L. Ciabattoni *et al.*, "Human indoor localization for AAL applications: An RSSI based approach," in *Italian Forum of Ambient Assisted Living* (Lecture Notes in Electrical Engineering), vol. 426. Cham, Switzerland: Springer, 2017, pp. 239–250.

[35] P. Pivato, L. Palopoli, and D. Petri, "Accuracy of RSS-based centroid localization algorithms in an indoor environment," *IEEE Trans. Instrum. Meas.*, vol. 60, no. 10, pp. 3451–3459, Oct. 2011.

[36] O. G. Adewumi, K. Djouani, and A. M. Kurien, "RSSI based indoor and outdoor distance estimation for localization in WSN," in *Proc. IEEE Int. Conf. Ind. Technol.*, Feb. 2013, pp. 1534–1539.

[37] D. Capriglione, L. Ferrigno, E. D'Orazio, V. Paciello, and A. Pietrosanto, "Reliability analysis of RSSI for localization in small scale WSNs," in *Proc. IEEE Instrum. Meas. Technol. Conf. (I2MTC)*, May 2012, pp. 935–940.

[38] A. Baldini *et al.*, "Room occupancy detection: Combining RSS analysis and fuzzy logic," in *Proc. IEEE 6th Int. Conf. Consum. Electron.*, Berlin, Germany, Sep. 2016, pp. 69–72.

[39] A. I. Kyritsis, P. Kostopoulos, M. Deriaz, and D. Konstantas, "A BLE-based probabilistic room-level localization method," in *Proc. Int. Conf. Localization GNSS (ICL-GNSS)*, Barcelona, Spain, Jun. 2016, pp. 1–6.

[40] S. Hotta, Y. Hada, and Y. Yaginuma, "A robust room-level localization method based on transition probability for indoor environments," in *Proc. Int. Conf. Indoor Positioning Indoor Navigat. (IPIN)*, Sydney, NSW, Australia, Nov. 2012, pp. 1–8.

[41] A. Corna, L. Fontana, A. A. Nacci, and D. Sciuto, "Occupancy detection via iBeacon on Android devices for smart building management," in *Proc. Design, Automat. Test Eur. Conf. Exhib.*, 2015, pp. 629–632.

[42] P. Barsocchi, A. Crivello, M. Girolami, F. Mavilia, and F. Palumbo, "Occupancy detection by multi-power Bluetooth low energy beaconing," in *Proc. Int. Conf. Indoor Positioning Indoor Navigat. (IPIN)*, Sapporo, Japan, Sep. 2017, pp. 1–6.

[43] L. M. Candanedo and V. Feldheim, "Accurate occupancy detection of an office room from light, temperature, humidity and CO_2 measurements using statistical learning models," *Energy Buildings*, vol. 112, pp. 28–39, Jan. 2016.

[44] F. Grossi, V. Bianchi, A. Losardo, G. Matrella, I. De Munari, and P. Ciampolini, "A flexible framework for ambient assisted living applications," in *Proc. IASTED Int. Conf. Assistive Technol. (AT)*, 2012, pp. 817–824.

[45] *ZigBee Alliance Website*. Accessed: May 2018. [Online]. Available: http://www.zigbee.org/

[46] V. Bianchi, C. Guerra, M. Bassoli, I. De Munari, and P. Ciampolini, "The HELICOPTER project: Wireless sensor network for multi-user behavioral monitoring," in *Proc. Int. Conf. Eng., Technol. Innov. (ICE/ITMC)*, Funchal, Portugal, Jun. 2017, pp. 1487–1496.

[47] *Fractus Compact Reach Xtend Datasheet*. Accessed: Nov. 2017. [Online]. Available: http://www.fractusantennas.com/compact-reach-xtend/

[48] *Joahnson Technology Balun 2450BM15A0002 Datasheet*. Accessed: Nov. 2017. [Online]. Available: https://www.johansontechnology.com/datasheets/baluns-matched/2450BM15A0002.pdf

[49] F. Montalto, C. Guerra, V. Bianchi, I. De Munari, and P. Ciampolini, "MuSA: Wearable multi sensor assistant for human activity recognition and indoor localization," in *Ambient Assisted Living* (Biosystems & Biorobotics), vol. 11. Cham, Switzerland: Springer, 2015, pp. 81–92.

[50] V. Bianchi, F. Grossi, I. De Munari, and P. Ciampolini, "MuSA: A multisensor wearable device for AAL," in *Proc. Federated Conf. Comput. Sci. Inf. Syst.*, Szczecin, Poland, Sep. 2011, pp. 375–380.

[51] T. Fawcett, "An introduction to ROC analysis," *Pattern Recognit. Lett.*, vol. 27, no. 8, pp. 861–874, Jun. 2006.

Valentina Bianchi received the B.Sc. and M.Sc. degrees (*summa cum laude*) in electronic engineering and the Ph.D. degree from the Department of Information Engineering, University of Parma, Parma, Italy, in 2003, 2006, and 2010, respectively.

From 2012 to 2017, she was a Technical Assistant with the University of Parma, where she has been a Research Assistant with the Department of Engineering and Architecture since 2017. She participated in several national and international projects. She has authored or co-authored over 30 papers in technical journals or proceedings of international conferences. Her current research interests include digital system design and wireless sensor networks.

Paolo Ciampolini received the bachelor's degree (*summa cum laude*) in electronic engineering from the University of Bologna, Bologna, Italy, in 1983, and the Ph.D. degree in electronics and computer sciences in 1989.

From 1990 to 1992, he was a Research Assistant with DEIS, University of Bologna. From 1992 to 1998, he was an Associate Professor with the University of Perugia, Perugia, Italy. From 1998 to 2001, he was an Associate Professor of electronics with the University of Parma, Parma, Italy, where he has been a Full Professor since 2001 and also an in charge of electronics fundamentals and digital design courses. From 2001 to 2008, he was the Chairman of the Board of Electronics with the Engineering Faculty, University of Parma. He has authored or co-authored over 180 papers in technical journals or proceedings of international conferences. He is currently involved in some projects in the area of active aging, in the framework of European AAL-JP and H2020 programs. His current research interests include the physical and numerical modeling of semiconductor devices, the design and optimization of solid-state radiation sensors, digital circuit design, and assistive technology devices.

Ilaria De Munari received the Electronic Engineering degree and the Ph.D. degree in information technologies from the University of Parma, Parma, Italy, in 1991 and 1995, respectively.

In 1997, she joined the Department of Information Engineering (presently the Department of Engineering and Architecture), University of Parma, as a Research Assistant, where she has been an Associate Professor of electronics since 2004. She was involved in several activities related to assistive technologies, managing some projects in the framework of Ambient Assisted Living Joint Programme in collaboration with other European partners. She is involved in research activities related to the design of electronic systems for Human Activity Recognition, and in general, for healthcare problems based on microcontroller and field-programmable gate array solutions. She has authored or co-authored over 100 papers in technical journals or proceedings of international conferences. Her current research interests include the reliability of semiconductor devices and the design of low-power digital integrated circuits and power-aware applications, cooperating to several national and international projects.